J Electroceram (2006) 16: 159–165
DOI 10.1007/s10832-006-6243-2

Effects of molten salt synthesis (MSS) parameters on the morphology of $Sr_3Ti_2O_7$ and $SrTiO_3$ seed crystals

E. K. Akdogan · Raymond Edwin Brennan · Mehdi Allahverdi · Ahmad Safari

Received: 11 June 2004 / Revised: 26 October 2005 / Accepted: 11 November 2005

Abstract A two-step molten salt synthesis process was utilized to fabricate $Sr_3Ti_2O_7$ and $SrTiO_3$. High aspect ratio $SrTiO_3$ seed crystals were developed by optimizing processing conditions such as temperature, salt-to-oxide ratio, and flux type in a systematic fashion. $Sr_3Ti_2O_7$ seeds were synthesized at temperatures ranging from 1050–1350°C, using salt-to-oxide ratios of 3:1, 1:1, and 1:3, and various salt types, including NaCl, KCl, and a 1:1 combination of NaCl and KCl. $Sr_3Ti_2O_7$ seeds synthesized at 1250°C with a 1:1 salt-to-oxide ratio in 100% NaCl salt resulted in a majority of higher aspect ratio platelets and elongated platelets as opposed to lower aspect ratio cubic-like and tetragonal-like morphologies. The seeds were 10–40 μm in length with aspect ratios of highly elongated platelets as high as 25:1. A second MSS step was used to synthesize $SrTiO_3$ seeds of the proper composition by TiO_2 addition to the $Sr_3Ti_2O_7$ seeds and heat treatment at 1100°C. These studies showed that highly anisotropic $SrTiO_3$ seeds could be produced at 1250°C using a 1:1 salt-to-oxide ratio in 100% NaCl flux. XRD studies of the resulting $SrTiO_3$ seeds revealed that the increase in aspect ratio for these particular seeds also resulted in the enhancement of (200) peaks, which are of major interest for texturing of PMN-PT.

Keywords Molten salt synthesis · $Sr_3Ti_2O_7$ · $SrTiO_3$ · Seed crystals · Texturing

E. K. Akdogan · R.E. Brennan · M. Allahverdi · A. Safari (✉)
Department of Materials Science and Engineering,
Rutgers University, 607 Taylor Road,
Piscataway, NJ 08854-8065, USA
e-mail: safari@rci.rutgers.edu

1. Introduction

Molten salt synthesis (MSS) is a technique by which millimeter-size seed crystals can by synthesized at low temperatures. It is a well-established fact that the reaction rates and diffusion kinetics are sluggish in low-temperature processes because of limited thermal activation. A typical countermeasure to overcome such barriers is to increase the processing temperature so as to increase reaction and mass transport rates, thereby reducing the time scales involved in a given process [1]. A good example to such an approach is the so-called mixed oxide route—a process based on solid-state diffusion. MSS, on the other hand, takes advantage of the much higher mass transport rates attainable in a melt, thereby enabling one to carry out the synthesis at modest temperatures at a reasonable rate [1]. The three main stages of MSS include: (i) mechanical mixing of the salt and oxides, (ii) melting of the salt and homogenization of the constituents in the melt, and (iii) heat treatment to effect the nucleation and growth of the desired phase [2]. The two fundamental requirements for MSS are: (i) the judicious choice of proper oxides that will ultimately form the desired solid solution in the end, and (ii) the use of suitable lower melting temperature fluxes, which will promote the reactions to occur at a low temperature. The choice of the fluxes is critical since the salts should not react with what is being synthesized (negligible solid solubility in the oxides), should be easy to remove after the process is completed, and should have low melting temperatures relative to the formation temperatures of the products [1]. Of utmost importance are MSS processing parameters such as the ratio of salt-to-oxide powder, the type of salt or salt mixture, the initial particle size of the starting materials, and the synthesis temperature and dwell time of the heat treatment as they dictate the final particle size, morphology and aspect ratio of the product(s) (hereafter seeds) [2].

High aspect ratio seeds are desired for *in-situ* templated grain growth (TGG), which involves aligning of the seed crystals in a matrix and a subsequent heat treatment to enhance texturing along a specific crystallographic direction. By the proper choice of the texturing direction, one can asymptotically approach single crystal properties in a given material, and at the same time bypass the difficulties associated with single crystal growth processes, especially in the case of Pb-based ferroelectric oxides. However, it is imperative that the aspect ratio of the seed crystals be maximized to: (i) provide better alignment in the matrix during forming, and (ii) have maximum thermodynamic driving force along a specific crystallographic axis [3].

Anisotropic and ⟨100⟩-oriented $SrTiO_3$ seed crystals with average lengths of ∼10–30 μm and a thickness of ∼2–5 μm (average aspect ratios ranging from 2:1 to 15:1) have previously been fabricated by a two-step MSS reaction [4–8]. Tetragonal $Sr_3Ti_2O_7$ seeds were synthesized in the first MSS step, and used to grow cubic $SrTiO_3$ in molten potassium chloride salt in the second MSS step [4]. These $SrTiO_3$ seed crystals have been utilized as templates for texturing of sodium bismuth titanate, $(Na_{1/2}Bi_{1/2})_{0.945}Ba_{0.055}TiO_3$ [9], and lead magnesium niobate-lead titanate, $Pb(Mg_{1/3}Nb_{2/3})O_3$-$PbTiO_3$ [6–11]. In the previous studies, the effects of MSS parameters such as temperature, salt-to-oxide ratio, and flux type on the morphology of $Sr_3Ti_2O_7$ and $SrTiO_3$ seed crystals have not been investigated in a systematic fashion. Therefore, the purpose of this study is to provide a quantitative account of the effects of such MSS processing parameters on seed crystal morphology so as to establish a solid footing for optimized TGG of ferroelectric materials.

2. Experimental

$SrCO_3$ (99.9% Aldrich) and TiO_2 (>99% Aldrich, predominantly rutile) were mixed in a 3.1:2.0 molar ratio (2.86:1.0 weight ratio) in accordance to the first MSS reaction represented by:

$$3SrCO_3 + 2TiO_2 \rightarrow Sr_3Ti_2O_7 + 3CO_2 \quad (1)$$

The $SrCO_3$ and TiO_2 were ball milled in ethyl alcohol for 24 h. After mixing the oxides, salts of either KCl, (99.0–100.0% Alfa Aesar), NaCl (99.0% Alfa Aesar), or a 50:50 weight % mixture of both were added, and an additional 24-h mixing step was employed. Salts such as potassium chloride (KCl) and sodium chloride (NaCl) have melting temperatures of ∼780 and ∼800°C; respectively. They serve as good low temperature melting fluxes that allow high mobility of oxides. The effect of salt-to-oxide ratio (S/O) was analyzed by varying it as 3:1, 1:1, and 1:3. Upon mixing, the constituents were dried overnight, placed into an Al_2O_3 crucible, and sealed. The mixture underwent heat treatment at a rate of 500°C/h, with maximum temperatures ranging from 1050 to 1350°C. The mixture was then cooled at 180°C/h to room temperature, after an isothermal soak at the maximum temperature for 6 hours duration. The fused mixture was slowly dissolved and stirred in boiling water over a series of washing steps (10–15 in total) in order to remove the salt, which was followed by a series of ultrasonic washing steps (5–10) in isopropyl alcohol so as to separate the coarse $Sr_3Ti_2O_7$ seeds (∼10–30 μm) from the fine seeds (1–5 μm). The coarse seeds were then analyzed by X-ray diffraction (XRD) for qualitative phase analysis to confirm the identification of the seeds as $Sr_3Ti_2O_7$, and by scanning electron microscopy (SEM) to study the aspect ratios and morphologies of the seeds grown under different conditions.

The coarse $Sr_3Ti_2O_7$ seed crystals were prepared for a second MSS step, based on the reaction:

$$Sr_3Ti_2O_7 + TiO_2 \rightarrow 3SrTiO_3 \quad (2)$$

by adding a 1.0:1.1 molar ratio (5.36:1.0 weight ratio) of $Sr_3Ti_2O_7$ to TiO_2. The seeds and powder were mixed for 24 h in isopropyl alcohol. The type of flux and S/O ratio were kept the same as in the first MSS step. The oxide and salt(s) were again mixed for 24 h on a ball mill. After drying, the constituents were added to an Al_2O_3 crucible, and underwent heat treatment at a rate of 600°C/h up to 1200°C for 4 h. The seeds went through 10–15 washing, and 5–10 ultrasonication steps to separate the fine seeds from the coarse ones as before. The remaining coarse seeds were examined with X-ray diffractometry and scanning electron microscopy (SEM) as before.

3. Results and discussion

The three processing parameters that were systematically varied during processing to analyze their effects on aspect ratio and morphology were the temperature of heat treatment, the salt-to-oxide ratio (S/O), and the type of flux used for the reaction. Specifically, these processing parameters were altered during the synthesis of $Sr_3Ti_2O_7$ seed crystals in the first MSS step so as to investigate any possible changes in the morphology and aspect ratio of the grown seeds as that dictates the final morphology. All of the other processing conditions remained equal, i.e. ceteris paribus.

3.1. Effect of temperature

Four batches of $Sr_3Ti_2O_7$ seeds crystals were prepared with 100% KCl flux and 1:1 salt-to-oxide ratio, with all other processing steps remaining equal except for the maximum

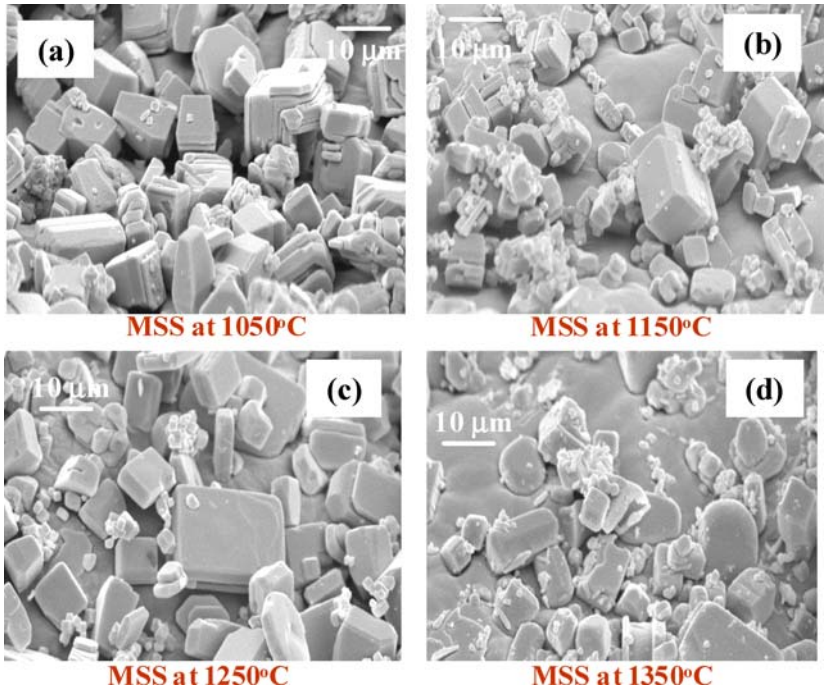

Fig. 1 $Sr_3Ti_2O_7$ seeds synthesized at different temperatures

temperature of heat treatment. The batches of seeds were synthesized at 1050, 1150, 1250°C, and 1350°C. Figure 1 shows SEM micrographs of the seeds as a function of processing temperatures. The lower temperature batches heat-treated at 1050°C and 1150°C showed 10–20 μm grown $Sr_3Ti_2O_7$ seed crystals with almost exclusively cubic-like and tetragonal-like morphologies, as shown in Figs. 1(a) and (b), respectively. The seed crystals that were synthesized at 1250°C started to show evidence of platelet morphologies (Fig. 1(c)), with an increase in the number of seeds with higher aspect ratios ~6:1 (average ~12 μm length and ~2μm thickness). In the samples synthesized at 1350°C, one observes that the edges of the seeds became rounded and indicated the beginning of a decrease in the high aspect ratio morphology (Fig. 1(d)).

The morphology and estimated aspect ratio (ξ_e) of the seeds that were synthesized at the temperatures indicated and discussed above is summarized in the schematic depicted in Fig. 2. The aspect ratio of pseudo-cubic and pseudo-tetragonal seeds was found to be ~1:1 and ~3:1, respectively. These types of morphologies make it difficult to obtain well-aligned seeds under the action of a shear force during forming processes such as tape casting or solid freeform fabrication [12]. It follows from the SEM study that the best temperature range for producing higher aspect ratio $Sr_3Ti_2O_7$ seed crystals is in the vicinity of 1250°C. However, when the temperature is increased further, the aspect ratio diminishes. The decrease in aspect ratio for temperatures above 1250°C can be attributed to the loss of potassium and sodium via evaporation from the system, thereby adversely changing the solubility of

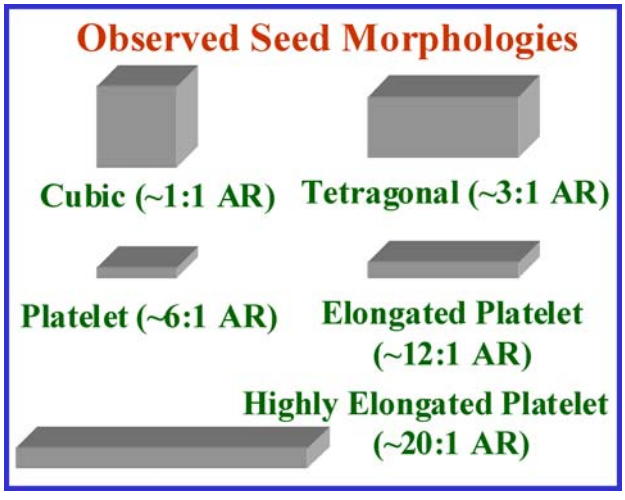

Fig. 2 Schematic of the observed morphologies in grown $Sr_3Ti_2O_7$ seeds. (AR: aspect ratio)

the oxides in the melt. As the initial composition of the flux as well as the salt/oxide ratio would change due to volatilization at such high temperatures, one expects the morphology of the seeds to be affected accordingly.

3.2. Effect of salt-to-oxide ratio

Figure 3 shows representative samples of $Sr_3Ti_2O_7$ seed crystals synthesized at 1250°C in 100% KCl flux, using various S/O ratios ranging in the order 3:1, 1:1, and 1:3. The seeds in Fig. 3(a) (S/O=1:1) were produced under the same conditions

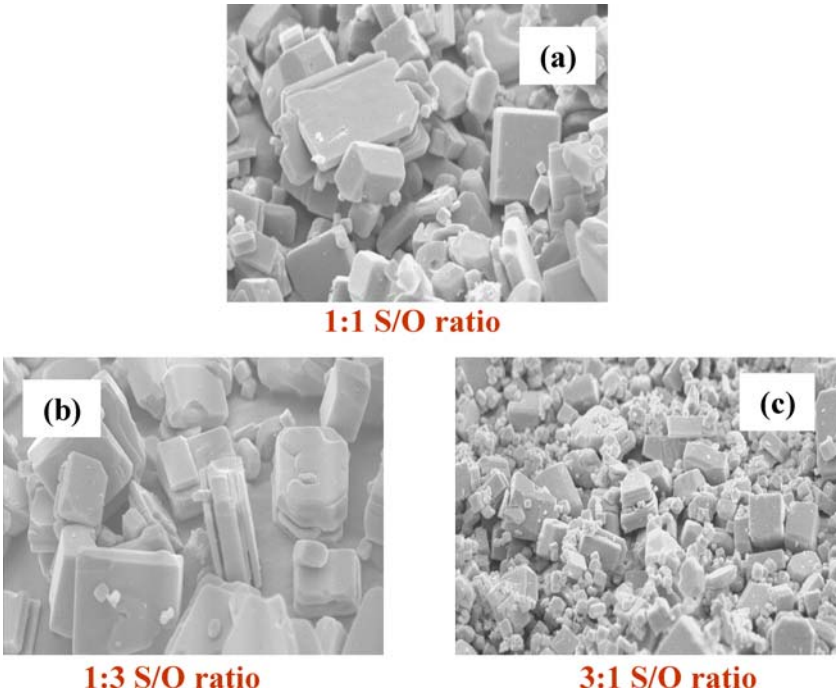

Fig. 3 $Sr_3Ti_2O_7$ seeds synthesized with different salt-to-oxide ratios at 1250°C

as the seeds depicted in Fig. 1(c). Comparing the two figures, one observes a mixture of higher aspect ratio platelet seeds and seeds with pseudo-cubic as well as pseudo-tetragonal morphologies. In going to 3:1 and 1:3 S/O ratio, however, one observes a pronounced change in the morphology of the seeds as shown in Figs. 3(b) and (c). The seeds synthesized at a 1:3 ratio, which are obtained from batches containing more oxide than salt content, do not exhibit the desired high ξ_e. In such batches, the seeds grew into each other, giving the appearance of a stacked or layered structure, as shown in Fig. 3(b). It is appearent that the amount of molten flux in the crucible was not enough to separate the growing seeds from each other, so they could not grow as individual seed crystals. Platelet seeds could not be mechanically separated. As such, these seeds were essentially aggregates with low aspect ratio.

The seeds synthesized with 3:1 salt-to-oxide ratio contained excessive flux so that 10–15 washing steps were not sufficient to remove the salts from the oxides. In an effort to separate out the salts and fine $Sr_3Ti_2O_7$ seed crystals, the washing and ultrasonication steps were doubled. However, that did not suffice to isolate the majority of coarse seeds from the salts and the fine seeds. In Fig. 3(c) the fine seeds (1–3 μm) that could not be separated from the remainder of the batch even after doubling the number of washing and ultrasonication steps are shown. These steps are critical for minimizing the amount of salt since the dissolution of even minute monovalent cations (K+ and Na+ in this case) in the host lattice during the subsequent TGG may degrade the dielectric properties and impart accelerated aging [2]. Some of the coarse 3:1 seeds could be recovered from the synthesized batches, and were analyzed by SEM. No aggregation among the coarse seeds has been observed as in the case of 1:3 S/O seeds. Furthermore, SEM studies indicated that the coarse 3:1 S/O seeds were of high aspect ratio.

It follows from the phenomenological observations discussed above that a low salt content is advantageous for practical purposes since it is easier to separate out the synthesized seeds after cooling. A higher salt content produces an increase in seed size and aspect ratio. That, in turn, is due to an increase in the mean particle separation in the melt, leading to an extended growth without the hindrance of the concomitant growth of surrounding particles or the fusion of particles onto each other. On the other hand, a higher flux ratio also leads to a bimodal seed size distribution, in which the separation of coarse and high ξ_e seeds becomes difficult. Based on the aforementioned experimental results, it can be concluded that 1:1 S/O ratio is the best compromise. It produces seeds with acceptable aspect ratio ($\xi_e \sim$ 6:1), while maintaining easy separation of coarse seeds (10–20 μm) from fine ones (1–3 μm). Although the seed size is still bimodal, the fraction of fine seeds (~0.40) is appreciably lower than that of large seeds.

3.3. Effect of flux type

The third parameter analyzed was the effect of flux type on the final morphology and aspect ratio of $Sr_3Ti_2O_7$ seeds. Based on the effect of temperature and salt-to-oxide ratio study,

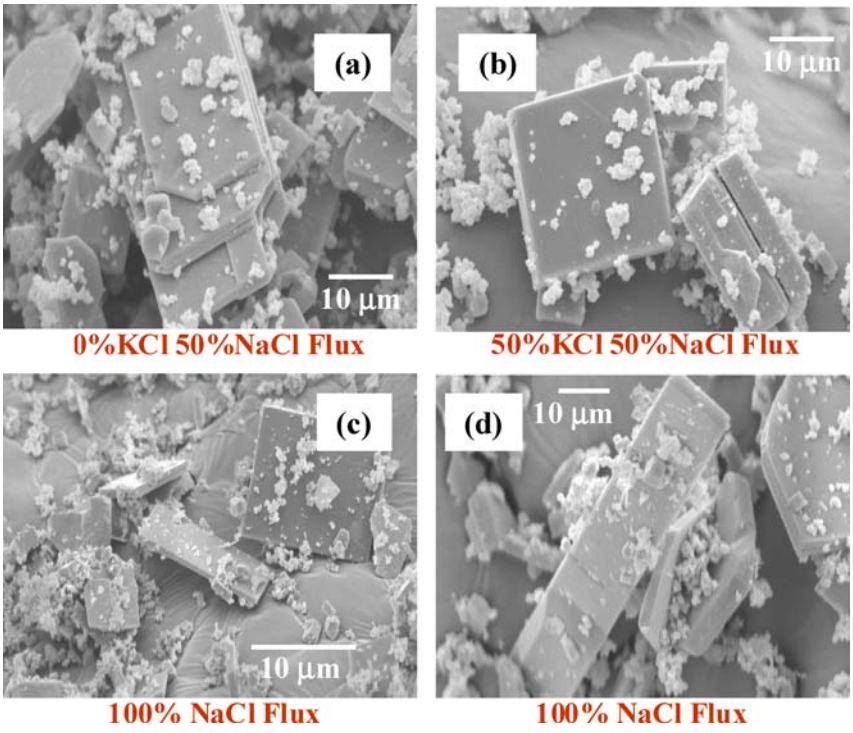

Fig. 4 $Sr_3Ti_2O_7$ seeds synthesized with different fluxes at 1250°C

all seed crystals were synthesized with a salt-to-oxide ratio of 1:1 at 1250°C. Then, 100% KCl flux, 50%KCl:50%NaCl and 100% NaCl fluxes were utilized. The seeds synthesized using 100% KCl flux with 1:1 salt-to-oxide ratio at 1250°C typically showed a mixture of cubic-like, tetragonal-like, and platelet-like seed crystals, which was consistent with previous seeds grown under the same conditions. With the addition of NaCl to KCl so as to obtain a 50% equi-molar flux mixture, a major improvement in the aspect ratio was observed. SEM studies showed that a greater number of platelets of $Sr_3Ti_2O_7$ were grown, as compared to cubic-like and tetragonal-like seed crystals as in the case for 100% KCl flux. Figures 4(a) and (b) demonstrate the improvement, showing elongated platelets with aspect ratios in the range of ∼10:1 to 15:1. The submicron particles in the SEM images are the result of insufficient washing of these samples, but this problem was easily corrected by adding several more washing and ultrasonication steps to the post-synthesis process. When the flux was changed to 100% NaCl, the overwhelming majority of grown seeds possessed a tabular morphology, and the average size of the seeds had further increased as shown in Figs. 4(c) and (d). A small percentage of the $Sr_3Ti_2O_7$ seeds showed aspect ratios as high as ∼20:1 to ∼25:1 (∼50 μm length, ∼2 μm thickness). Both size and shape differences were evident as the flux was changed. In Fig. 5, the X-ray pattern of the $Sr_3Ti_2O_7$seeds as obtained after the first MSS step using 100% KCl and NaCl flux is shown, respectively. The phase of $Sr_3Ti_2O_7$ obtained therein is tetragonal (JCPDF Card #: 11-0663), and the experimentally observed intensities indicate an equi-partitioned [114] and [107] preferred orientation. No appreciable second phase is seen in the X-ray patterns.

Previous work has shown that the solubility relation between a given oxide and a flux is critical in dictating the rate of seed formation, its morphology and size [2, 13–16]. Specifically, the extent of supersaturation of the molten salt for a given oxide under isothermal conditions determines the final morphology as well as the size of the final seeds, i.e. the higher the supersaturation the higher the aspect ratio and size of seeds. It follows from this line of reasoning in conjunction with the experimental results obtained herein that the solubility of TiO_2 and $SrCO_3$ should be higher in NaCl than KCl, since larger seed crystals were synthesized from in molten salts containing NaCl flux for a given processing temperature and cooling rate [2].

3.4. Synthesis of $SrTiO_3$ seeds

After optimization of the morphology and aspect ratio of the grown $Sr_3Ti_2O_7$ seed crystals, the second MSS step was conducted and the proper separation steps were performed to synthesize $SrTiO_3$ seeds. $Sr_3Ti_2O_7$ seed crystals produced from 100% KCl, 50% KCl-50% NaCl, and 100% NaCl fluxes in the first MSS step were used to obtain $SrTiO_3$ in the second MSS step. Figures 6(a) and (b) show a comparison between $SrTiO_3$ seeds synthesized from 100% KCl and 100% NaCl fluxes, respectively. It is seen that there is a difference in size and shape of the resulting $SrTiO_3$ seeds, with the majority

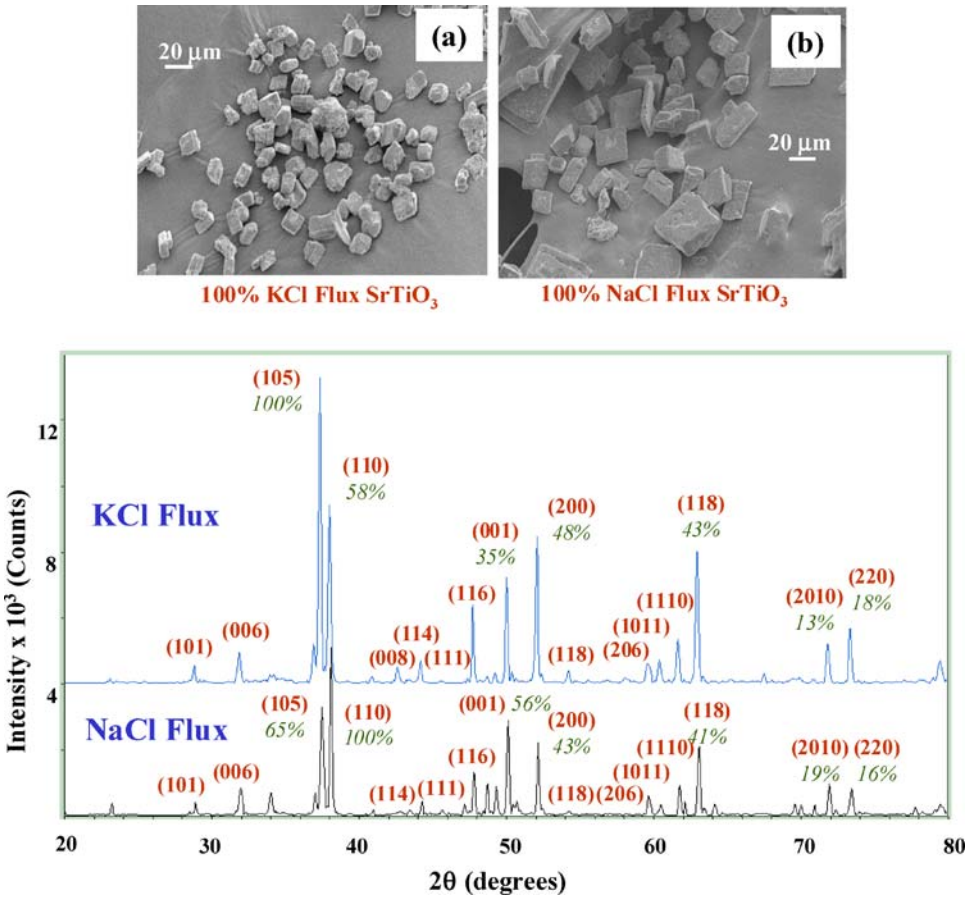

Fig. 5 Phase analysis of $Sr_3Ti_2O_7$ seed prepared from KCl and NaCl fluxes at 1250°C

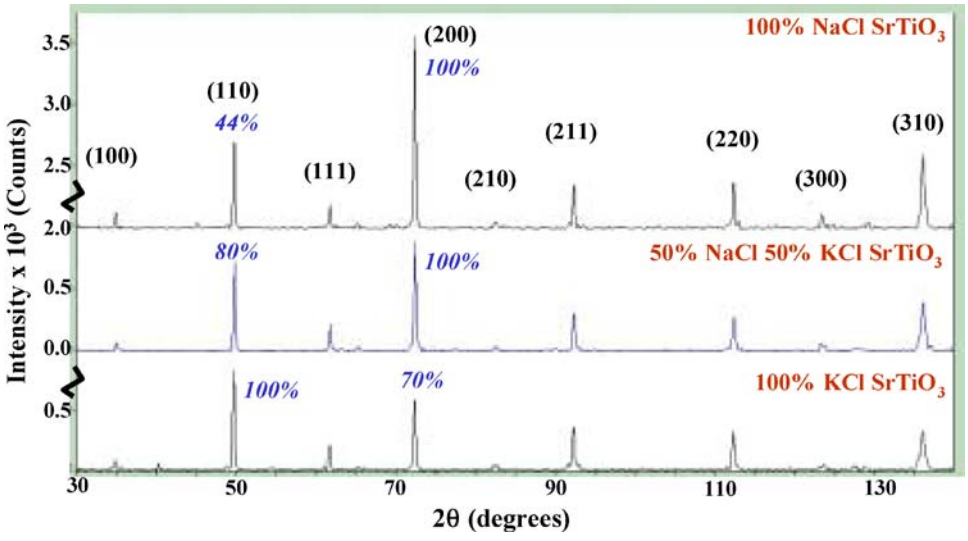

Fig. 6 X-ray comparison of $SrTiO_3$ seeds synthesized with different fluxes

of seeds from 100% KCl flux being ~10–15 μm in length, either a pseudo-cubic or pseudo-tetragonal morphology. The seeds obtained from 100% NaCl, on the other hand, were larger typically ~20–40 μm length and possess a platelet or elongated platelet morphology. It is interesting to note that the observed variation in seed size and morphology in $SrTiO_3$ parallels that of its precursor ($Sr_3Ti_2O_7$), indicating that the growth mechanism of such Sr^{+2} and Ti^{4+} oxides should be the same in KCl and NaCl melts in MSS.

X-ray studies not only confirmed that the seed crystals were characteristic of (100)-oriented $SrTiO_3$, but also a significant difference between the $SrTiO_3$ seeds grown from different fluxes, resulted in different preferred orientation. Figure 6 is a comparison of XRD spectra of $SrTiO_3$ seeds

grown from $Sr_3Ti_2O_7$ seeds, synthesized in either 100%KCl, 50%KCl:50%NaCl, or 100%NaCl fluxes. The samples were prepared for XRD by aligning a thin layer of $SrTiO_3$ seeds on the sample holder and performing a scan over 2θ values of 20-80°. The peak with the highest intensity for a standard polycrystalline $SrTiO_3$ powder sample (JCPDS PDF#35-0734) belongs to the (110) refection. In such patterns, the (200) peak is typically ∼50% of the intensity of the (110) peak. Using the first two strongest peaks as indicated above, we have examined the X-ray traces of the seeds and have determined that residual $Sr_3Ti_2O_7$ after the second MSS was very negligible. The main phase obtained by the use of three types of fluxes was identified as a cubic $SrTiO_3$ (JCPDF card # 35-0734) as shown in Fig. 6. The $SrTiO_3$ seeds crystals from 100% KCl showed the same peak trends, but there was evidence of some enhancement of the (200) peak, which was ∼70% of the highest intensity (110) peak. As the NaCl flux was added for the 50% KCl:50% NaCl $SrTiO_3$ sample, the (200) peak became the highest intensity peak. For the $SrTiO_3$ seeds grown from 100% NaCl $Sr_3Ti_2O_7$ seed crystals, this enhancement became even more evident, as the (110) peak was ∼44% of the highest intensity (200) peak. The reason for the enhancement of the (200) peak with increased NaCl content was a direct result of the change in morphology. Since the number of seeds with platelet morphology increased with NaCl content, and the faces of the platelets possessed an (h00) orientation [4, 5], the intensity collected from XRD showed an enhancement of the (200) peak. The (h00) intensities from seed crystals with cubic-like or tetragonal-like morphologies were not as strong. This is the same reasoning that should be taken into consideration with texturing of the $SrTiO_3$ seed crystals. With proper alignment of the higher aspect ratio seeds in a compatible polycrystalline matrix by shear force, there should be a higher degree of texturing in a specific crystallographic orientation, resulting in higher material properties.

4. Concluding remarks

$SrTiO_3$ seed crystals were synthesized by a two-step MSS process. In the first MSS step, $Sr_3Ti_2O_7$ seeds were produced. $SrTiO_3$ seeds were then synthesized using $Sr_3Ti_2O_7$ seeds as precursor in a second MSS step. During the synthesis of $Sr_3Ti_2O_7$ seeds, processing parameters such as the maximum MSS temperature, the salt-to-oxide ratio, and the type of flux were varied; and their effect on the aspect ratio and morphology of the seed crystals were assessed. The highest aspect ratio seeds were obtained in $Sr_3Ti_2O_7$ seeds that were synthesized with a 1:1 salt-to-oxide ratio in 100% NaCl flux at 1250°C produced, along with a small percentage of highly elongated platelets exhibiting an aspect ratio as high as 25:1. SEM studies of the (100)-oriented $SrTiO_3$ seed crystals synthesized from these $Sr_3Ti_2O_7$ seeds resulted in an increase in STO seed aspect ratio as confirmed by X-ray diffractometry where an enhancement in the (200) peaks of $SrTiO_3$ was observed and is attributed to the increase in NaCl content.

Acknowledgments The authors are thankful for the financial support provided by the Office of Naval Research.

References

1. M. Thirumal, P. Jain, and A.K. Ganguli, *Mater. Chem. Physi.*, **70**, 7 (2001).
2. K.H. Yoon, Y.S. Cho, and D.H. Kang, *J. Mater. Sci.*, **33**, 2977 (1998).
3. S. Kwon, E.D. Sabolsky, and G.L. Messing, *Handbook of Advanced Ceramics*, Elsevier Inc., (2003)
4. K. Watari, B. Brahmaroutu, G.L. Messing, and S. Trolier-McKinstry, *J. Mater. Res.*, **15**(4), 846 (2000).
5. T. Takeuchi, T. Tani, and T. Satoh, *Solid State Ionics*, **108**, 67 (1998).
6. S. Kwon, E.M. Sabolsky, G.L. Messing, and S. Trolier-McKinstry, in *Proceedings of the 10th US-Japan Seminar on Dielectric and Piezoelectric Ceramics*, Providence, RI, (2001), p. 327.
7. E.M. Sabolsky, Ph.D. Thesis, Pennsylvania State University, (2001).
8. H. Liu, X. Sun, Q. Zhao, J. Xiao, and S. Ouyang, *Solid-State Electronics*, **47**, 2295 (2003).
9. H. Yilmaz, G.L. Messing, and S. Trolier-McKinstry, in *Proceedings of the International Symposium of Applied Ferroelectrics*, (2000). p. 405.
10. M.M. Seabaugh, G.L. Cheney, K. Hasinska, W.J. Dawson, and S.L. Swartz, in *IEEE Proceedings of the International Symposium on the Application of Ferroelectrics*, (2000), p. 377.
11. M.M. Seabaugh, G.L. Cheney, K. Hasinska, A.M. Azad, S.L. Swartz, and W.J. Dawson, in *Proceedings of the 10th US-Japan Seminar on Dielectric and Piezoelectric Ceramics, Providence, RI*, (2001), p. 351.
12. A. Safari, S.C. Danforth, A. Bandyopadhyay, M.K. Agarwala, R. Van Weeren, N. Langrana, V. Jamalabad, and W. Priedeman, "SFF Fabrications Methods", US Patent No. 5,900,207 (1999).
13. A.M. Scotch, Ph.D. Thesis; Lehigh University (2002).
14. E.M. Sabolsky, A.R. James, S. Kwon, S. Trolier-McKinstry, and G.L. Messing, *Appli. Physi. Lette.*, **78**(17), 2551 (2001).
15. B. Brahmaroutu, G.L. Messing, S. Trolier-McKinstry, and U. Selvaraj, in *IEEE Proceedings of the International Symposium on the Application of Ferroelectrics*, (1996), p. 883.
16. E. Heifets, R.I. Eglitis, E.A. Kotomin, J. Maier, and G. Borstel, *Surf. Sci.*, **513**, 211 (2002).